applied sciences

MDPI

Article

Infill Variability and Modelling Uncertainty Implications on the Seismic Loss Assessment of an Existing RC Italian School Building

Gianrocco Mucedero [1], Daniele Perrone [2] and Ricardo Monteiro [1,*]

[1] University School for Advanced Studies IUSS Pavia, 27100 Pavia, Italy
[2] Department of Engineering for Innovation, University of Salento, 73100 Lecce, Italy
* Correspondence: ricardo.monteiro@iusspavia.it

Abstract: Past earthquake evidence has shown the high vulnerability of Italian school buildings, given by the extensive damage observed to structural and non-structural elements. Such vulnerability demonstrates the need to undertake a seismic risk assessment and reduction strategies for critical facilities and allocation of national funds for retrofit interventions to those regions where seismic risk is higher. To do so, Expected Annual Losses (EAL) are evermore considered one of the main seismic risk metrics, which can, however, be largely affected by the epistemic uncertainty that typically characterizes the material and geometrical properties of existing buildings, particularly masonry-infilled reinforced concrete (RC) ones. This paper investigates the implications of accounting for a thorough identification of sources and characterization of uncertainty in seismic loss estimates on the risk assessment of a typical Italian masonry-infilled RC school building. The variability in masonry infill properties and modeling assumptions, as well as the subsequent epistemic uncertainty, are explicitly considered in the loss estimation of the RC school building. Specifically, the impact on the expected annual loss ratio is quantified in terms of both structural and non-structural components, depending on the engineering demand parameter to which they are sensitive. The results show that, when considering the uncertainty related to the variability in masonry infills, higher loss ratios of up to 30% are obtained with respect to the available literature estimates.

Keywords: masonry infill variability modelling uncertainty; collapse fragility curve; expected annual losses; seismic risk assessment

Citation: Mucedero, G.; Perrone, D.; Monteiro, R. Infill Variability and Modelling Uncertainty Implications on the Seismic Loss Assessment of an Existing RC Italian School Building. *Appl. Sci.* **2022**, *12*, 12002. https://doi.org/10.3390/app122312002

Academic Editor: Omar AlShawa

Received: 19 October 2022
Accepted: 22 November 2022
Published: 24 November 2022

1. Introduction

Extensive damage and structural collapse observed in Italian school buildings during past seismic events have pointed out the need for seismic risk mitigation programs. These should identify the most vulnerable building typologies and reduce earthquake-related economic losses and casualties through adequate seismic retrofit strategies. The collapse of a school in San Giuliano di Puglia during the 2002 Molise earthquake in Italy, which caused 30 fatalities, is a key example of the seismic vulnerability of the existing Italian school building stock (Borzi et al. [1]). The vulnerability of existing public buildings is not only related to structural components but also to all the non-structural components within it that could cause fatalities and economic losses. Adequate seismic performance of non-structural components should indeed be achieved to ensure safe public buildings, as also pointed out in [2,3]. Simplified or advanced methodologies to assess the safety of non-structural components [4] would ensure a higher level of safety, avoiding dramatic events, such as the death of a student in a school building in Rivoli (Italy) [4] caused by the collapse of a classroom ceiling.

The need for a seismic risk identification scheme for Italian school buildings, comprising both structural and non-structural elements, becomes therefore evident. In line with this, the regional interventions for the infrastructural and seismic upgrading of school

buildings were approved by the decree (n° 943 23 December 2015) of the Italian Ministry of Education, University and Research, following years of dedicated research on the seismic vulnerability of Italian school buildings and the need to prioritize rehabilitation interventions. Some examples include the risk-management framework to prioritize rehabilitation interventions for Italian school buildings, proposed by Grant et al. [5] or the research project "Progetto Scuole", which carried out a comprehensive structural performance and retrofitting assessment of typical Italian school buildings, from a comprehensive database of approximately 49,000 school buildings [6]. Data related to structural behavior, as well as other features concerning non-structural component typologies and their quantities, were collected, allowing the identification of representative case-study school buildings in order to perform detailed seismic assessment and loss estimation studies.

Despite the very large amount of data that can be collected for detailed seismic assessments and economic loss estimation, the uncertainty related to the masonry infill properties is expected to significantly affect their seismic response and risk. Their full characterization and the definition of a mechanical model that represents their real behavior under seismic loads is particularly complex. Such associated uncertainty should thus be properly accounted for in the collapse assessment of existing structures when detailed nonlinear structural analysis methodologies are adopted. In this sense, the collapse assessment of existing structures should account for both aleatory and epistemic uncertainties: the former is quantified by means of a selected ground motion set, while the latter requires a set of model realizations [7–10], defined from a random variable set, to propagate the modeling uncertainty in the numerical analysis.

Several studies have investigated and quantified the dispersion in the seismic response of existing RC buildings due to epistemic uncertainty surrounding the RC members, whereas less attention was paid to the impact of the uncertainty related to both the premature shear failure of poorly detailed columns and the variability of masonry infill properties. Recently, O'Reilly and Sullivan [11], using the Correlated Latin Hypercube Sampling method proposed by Olsson et al. [12], have investigated the epistemic uncertainty of existing RC buildings built in Italy before the 1960s, with different structural configurations (bare, infilled, and pilotis frames). A reduction of the median collapse intensity when the modeling uncertainty was accounted for in the collapse assessment was noticed, and the dispersion due to epistemic uncertainty was seen to be higher for bare frames with respect to infilled frames. In another study, Choudhury and Kaushik [13] investigated the effects of uncertainties in seismic fragility assessment of Indian RC infilled frames, noticing a higher dispersion instead in the structural response of infilled frames with respect to the bare-frame counterparts.

The main shortcomings of the abovementioned research studies and available literature in the field can be attributed to how the variability surrounding the mechanical properties of the infills is accounted for and to the type of numerical model that is implemented. Specifically, despite the high level of uncertainty surrounding the masonry infill properties, constant mechanical and geometrical properties have been typically assumed. Regarding the formulations to define the hysteretic response of masonry infills adopted in previous studies, the three main needed parameters (formulation to define the backbone curve, the relationships to calculate the width of the equivalent strut, and the strength model of the infill) were often selected a priori without any consideration of the specificities of the considered masonry infill. Moreover, the numerical model and subsequent collapse assessment did not account for the possible shear failure of poorly-detailed RC columns, which could occur due to frame-infill interaction. This is also a consequence of modeling the masonry infills through a single-strut modeling approach [14,15].

With the above in mind, this study presents the seismic risk assessment of one of the aforementioned masonry-infilled RC school buildings, with a focus on the importance of the uncertainty surrounding the definition of the infill panels and the effects of modeling uncertainty on the expected seismic losses. The variability in masonry infill properties is accounted for through a macro-classification comprising five masonry infill typologies.

Their impact on both capacity curves and the selected engineering demand parameters (Interstorey Drift and Peak Floor Acceleration) is scrutinized, showing how a sound characterization of the mechanical properties of the masonry infills is needed to properly assess the building seismic response. The effect of a more comprehensive modeling characterization of the uncertainty on the loss assessment is also investigated by means of two sets of dispersion values. The impact on the expected annual loss ratio is finally quantified in terms of both structural and non-structural components, depending on the engineering demand parameter to which they are sensitive.

2. Research Methodology

The adopted research methodology is based on the uncertainty estimation approach recently proposed by Mucedero et al. [16], who further integrated the estimation of modeling uncertainty in existing buildings, using a case-study masonry-infilled RC frame from an extensive building stock [17], representative of existing RC frames built in Italy between 1970 and 1980. The approach adopted by Mucedero et al. [16] covers some important aspects that were unaddressed by previous research studies on this topic, namely:

(i) The variability around the mechanical properties of masonry infills was considered. Five masonry infill typologies, from weak to strong, classified according to their shear strength, were selected as representative of the masonry infill typologies used in RC buildings in Italy [18];
(ii) The single strut macro-modeling technique generally implemented in previous studies was replaced by the three-strut modeling approach proposed by Chrysostomou et al. [19]; this modeling approach enabled a better estimation of the local interaction between frame and infills and, consequently, a more trustworthy estimation of the shear and moment distribution in the surrounding RC frame, as also pointed out by Crisafulli et al. [14,15];
(iii) Adoption of a numerical model for RC members able to account for material and geometrical nonlinearity, flexible joints with likely shear failure, the behavior of poorly detailed and non-ductile RC frame members, premature shear failure, deficiencies in concrete core confinement due to stirrups spacing, and inelasticity concentrated in the structural element ends;
(iv) The shear response parameters of RC members, such as beams and columns, were treated as a source of uncertainty, highlighting the relevant impact of the shear failure of poorly detailed RC members in the seismic performance assessment of GLD buildings.

In line with the above, this study makes use of the improved epistemic uncertainty estimates provided by Mucedero et al. [16] to quantify the impact of modeling uncertainty on the loss assessment of an existing masonry-infilled RC school building in Italy, analyzed fully through a 3D numerical advanced model. The points briefly discussed below summarise the adopted research methodology (Figure 1):

1. A representative case-study school building was selected as representative of the RC school buildings in Italy, according to the main features characterizing the existing school building stock [6];
2. The macro-level classification of masonry infills outlined in Mucedero et al. [18] was used to account for the variability of the geometrical and mechanical properties of the masonry infills. This also allows us to investigate the impact of different masonry infill typologies on the capacity curves and on nonlinear time history response analysis, leading to the economic loss estimation related to different non-structural components;
3. On the structural model side, the choice of explicitly modeling the presence of openings was investigated to analyze its role in the estimation of fragility curves, considering two structural configurations: (i) completely infilled structural configuration, disregarding the presence of the openings, and (ii) partially infilled structural configuration, considering the presence of the openings, whose dimensions were set according to the original drawings of the school building;

4. The impact of a more comprehensive modeling uncertainty characterization on the loss assessment of the selected case-study school building was investigated by means of two sets of dispersion values: the first set includes the values proposed by O'Reilly and Sullivan [11], whereas the second one accounts for the values recently proposed by Mucedero et al. [16], to gauge the differences. The seismic loss estimates were then obtained, for both structural configurations, according to the FEMA P-58-2 [3] methodology. Each dispersion set was used in the FEMA P-58 [3] dedicated tool (PACT) when setting the modeling dispersion of both Peak Storey Drifts (PSD) and Peak Floor Accelerations (PFA) for each scenario/intensity to incorporate the epistemic uncertainties in the collapse fragility functions. The two sets of results were compared to understand the overall impact of epistemic uncertainty, including a wider variability on the infill properties and collapse modes, on the loss estimates in existing buildings.

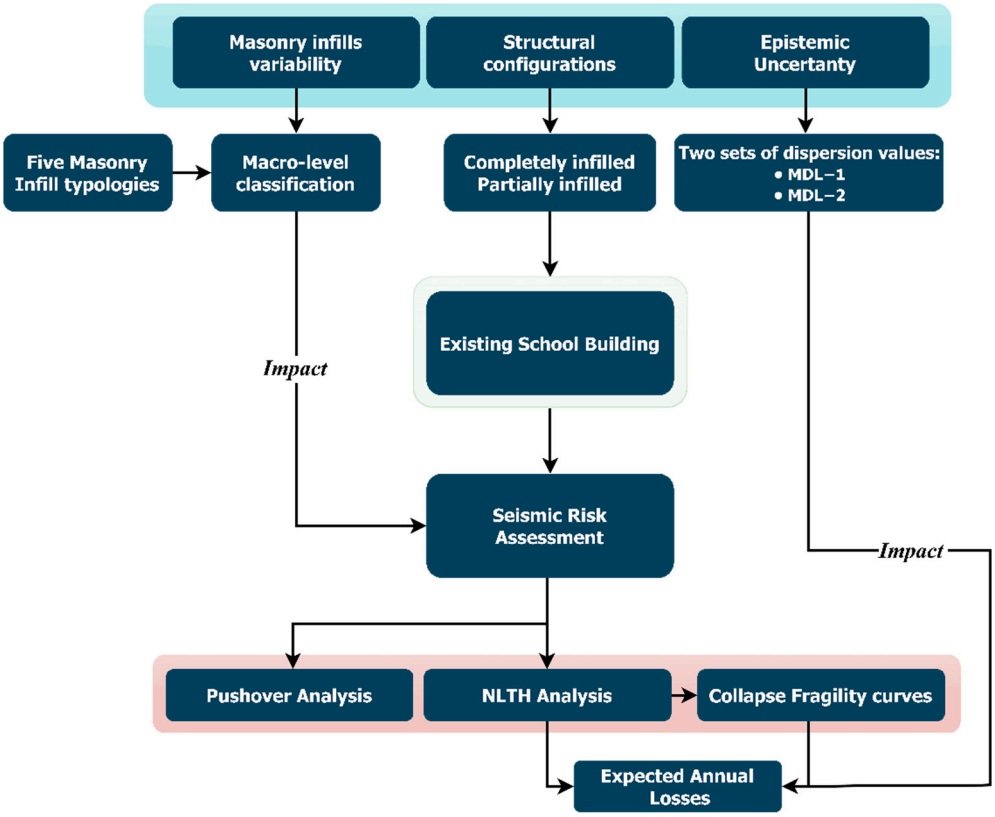

Figure 1. Research methodology.

3. Case-Study School Building

The analysis of the main features characterizing the aforementioned existing school building stock [6] has allowed us to identify a representative case-study school building, namely the primary school Antognini, located in Ancona (Italy). This school building was built in central Italy around the 1960s, and it is composed of three stories, including an underground level. The floor area is about 690 m^2, and the inter-story height is 3.83 m for the underground level and first story and 3.77 m for the second story. The longest side of the building is 57 m long, and the shortest is 12 m. The plan view and the south elevation of the school building are provided in Figure 2. In situ test reports made available during the survey of the building provided detailed information regarding material properties and reinforcement content for several structural elements; for those elements with no available steel reinforcement information, a reasonable value was estimated through a simulated design approach. Mean compressive strength of the concrete of 14.4, 10.8, and

8.7 MPa at the first (ground), second, and third stories, respectively, was obtained from the in situ tests; furthermore, the yield strength of the reinforcement bars was reported to be 381 MPa. Additional variability in the structural response at both global and local levels, deriving from a non-uniform distribution of the material strength at the member level or plan level [20], was not accounted for in the structural model.

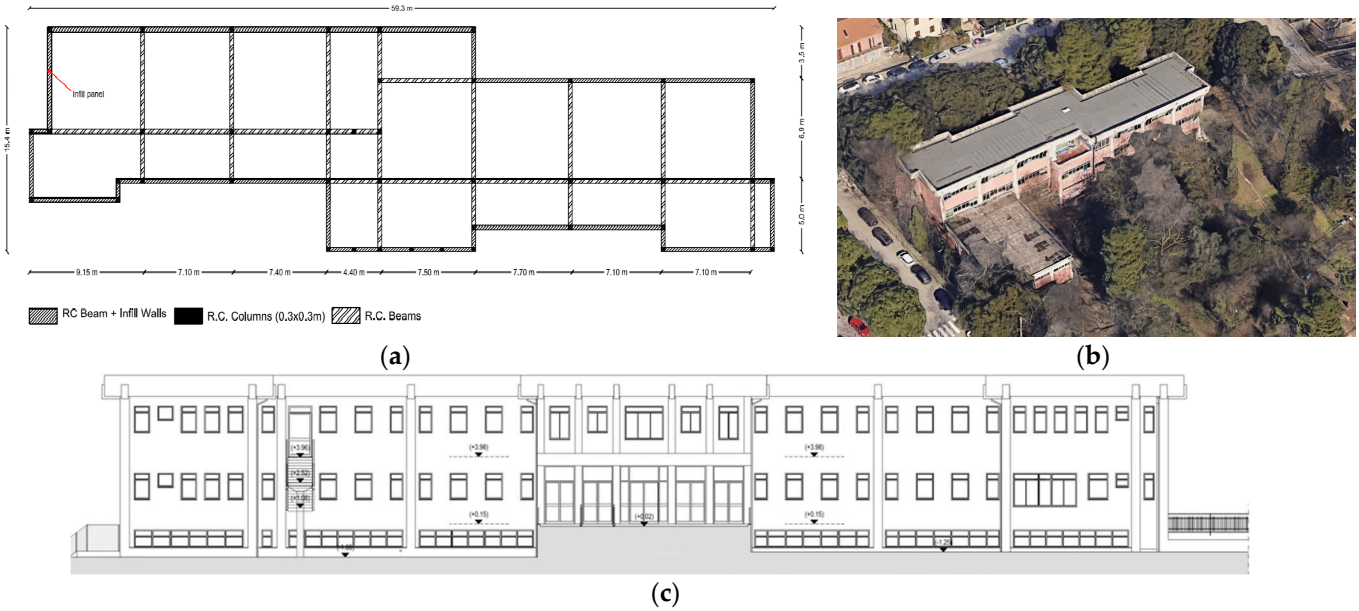

Figure 2. Case-study school building: (**a**) plan layout, (**b**) satellite view (Google Earth), and (**c**) longitudinal elevation.

The floor slab system, which was a hollow-core concrete structure, is the most common in Italy for RC buildings built in the 1960s, and, considering the thickness of the reinforced concrete slab on top of the hollow bricks, it was assumed as fully rigid.

3.1. Numerical Modeling, Seismic Hazard, and Records Selection

An advanced nonlinear numerical model was developed to assess the seismic response of the case study school building, which was built around 1960–1970 and designed for gravity loads only, which likely anticipates relevant structural vulnerability due to the lack of seismic provisions. To account for potential structural deficiencies generally found in similar RC buildings in Italy, the modeling approach proposed by O'Reilly et al. [21] and Perrone et al. [22] for older RC frames was followed, as shown in Figure 3.

The numerical model was developed using OpenSees [23], which integrates the structural behavior of flexural elements and joints. The flexural elements (i.e., beams and columns) were modeled through force-based beam-column elements with a modified Radau plastic hinge integration scheme, as suggested by Scott and Fenves [24]. Likewise, to capture the nonlinear behavior of joints, a zero-length spring coupled with a rotational hinge was adopted. Although the shear behavior of flexural elements was considered elastic, a post-processing analysis was carried out to determine any possible shear failure, similar to the approach adopted by Carofilis et al. [25]. Masonry infills were modeled using a single-equivalent-strut model, which reproduces the infill panel through one diagonal, compression-only nonlinear truss element for each direction. To account for the potential shear failure of columns and beams, as well as to capture the increment in the lateral stiffness and potential torsional modal behavior, the stair systems were modeled using a series of elastic frame elements. Moreover, the school building model foresaw a rigid floor slab, and second-order geometry effects (P-Δ) were taken into account. Regarding damping, 5% tangent stiffness proportional to Rayleigh damping at the fundamental periods was adopted.

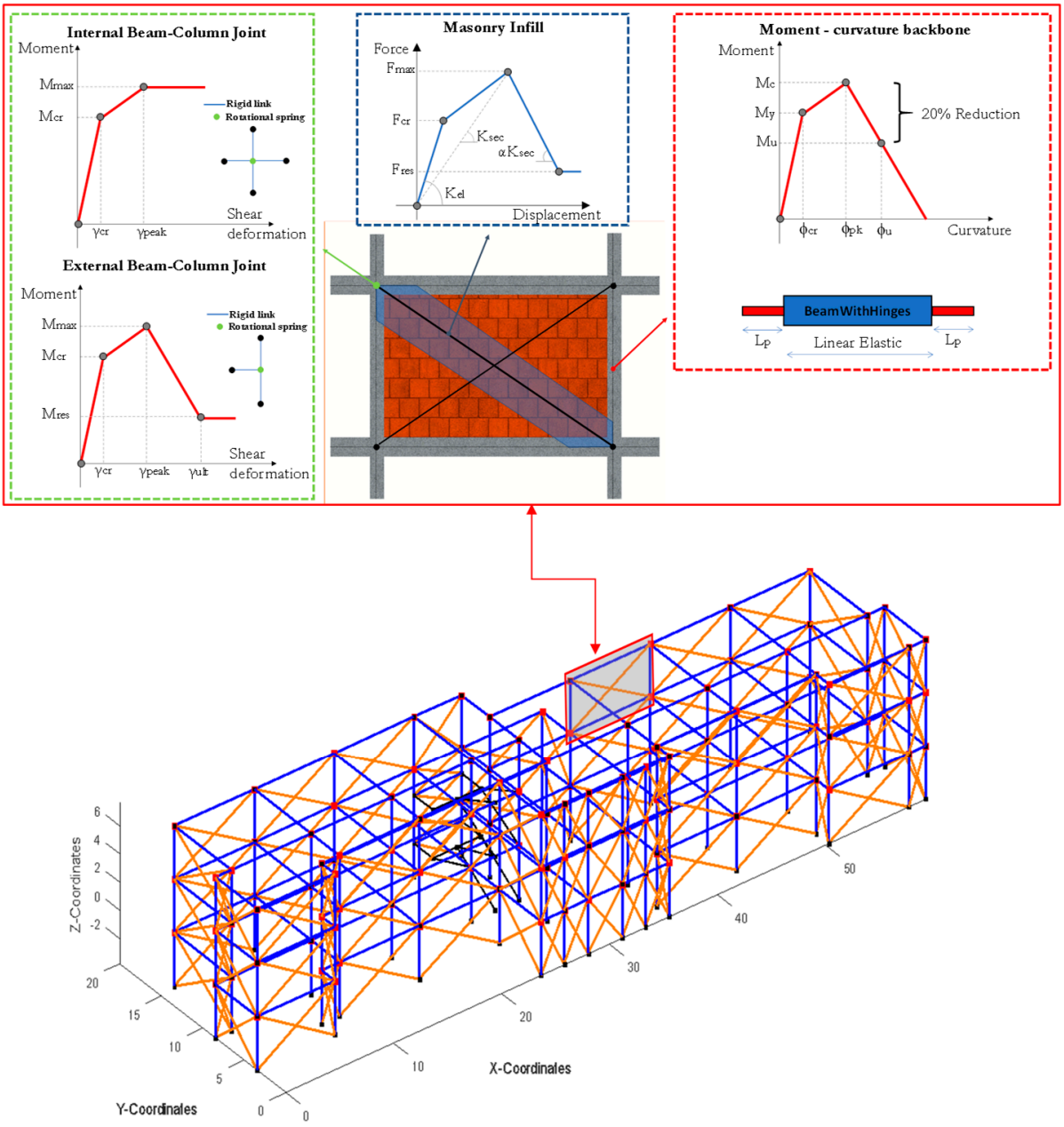

Figure 3. Case–study school building model in OpenSees [23] and illustration of the numerical modeling approach for masonry infill, frame elements, and beam–column joints.

It is worth mentioning that the school building analyzed herein was equipped with an advanced structural monitoring system aimed at continuous dynamic system identification through ambient vibration acquisitions, and the developed numerical model was validated in O'Reilly et al. [26], using ambient vibration acquisition data.

OpenQuake [27] was used to perform seismic hazard computations. The analysis is based on the SHARE Project [28] source model and the ground motion model proposed by Boore and Atkinson [29]. The hazard curve in terms of the spectral acceleration corresponding to the AvgSa (0.1:0.1:2.0 s) for the city of Ancona (Italy) [30,31] is shown in Figure 4a. A total of 25 pairs of ground motion records in two horizontal components were selected, for each of the ten intensity measure levels (IM levels), from the PEER NGA-West database [32]. For this purpose, any other ground motion record database, such as a European one [33], could have been used. Figure 4b illustrates the target conditional spectra (CS) for IM level 6 (close to Life Safety limit states (NTC 2018 [34]) for the site of interest, together with the

25 individual record spectra. More details on the record selection procedure are provided by Kohrangi et al. [30,31].

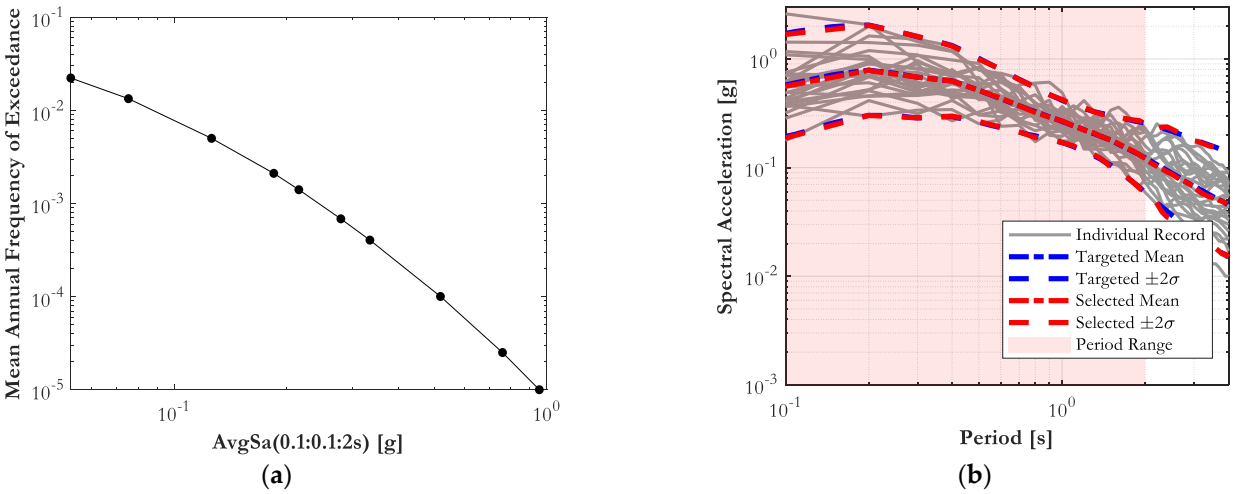

Figure 4. (**a**) Hazard Curve at the site of the school building; (**b**) target spectra for CS(AvgSa) [30,31] at IM level 6 together with the 25 selected individual records.

3.2. Variability in the Masonry Infill Mechanical Properties

In the past, only the structural components were involved in the design process, and consequently, the potentially aggravating effect of masonry infills on the RC frames (e.g., premature shear failure of the columns due to the interaction with the surrounding frames) was neglected. In contrast, past earthquake evidence demonstrated the relevant influence of masonry infills on the global and local behavior of RC buildings. The characterization of the mechanical properties of masonry infills and the definition of a mechanical model that represents their real behavior under seismic loads is particularly elaborate, as it depends on numerous factors (e.g., manufacturing techniques, compressive strength of bricks and mortar, brick with vertical or horizontal holes). Such complexity is further increased when existing buildings are to be analyzed, for which there is no sufficient information regarding the mechanical properties of the infills or when the results of in-situ tests on masonry infills, if any, are not easily available.

To account for these sources of uncertainty, the macro-level distinction of infill types proposed by Mucedero et al. [20] was used herein based on the results of experimental studies [33–35]. Accordingly, five masonry infill typologies, from weak to strong, classified according to their shear capacity, were thus selected as representative of the masonry infills typically present in RC buildings in Italy and other Mediterranean countries [36]. The choice of using the shear capacity as a parameter to distinguish between different masonry infill typologies is supported by numerical research studies [37], which noted that for existing buildings without seismic detailing, the maximum shear capacity of infills significantly affects both the overall seismic response and could cause the premature shear failure of RC columns. Table 1 reports the main properties of the selected typologies. To define the most consistent numerical modeling approach for each masonry infill typology, as discussed in detail in Mucedero et al. [18], the main parameters affecting the hysteretic behavior were identified. The most common formulations available in the literature were investigated (i.e., the strut width relationships, the formulations to account for the presence of openings, failure mechanism models, and the formulations to define the backbone curve).

Table 1. Material properties of the selected masonry infill types.

Parameters	Type 1 [36]	Type 2 [35]	Type 3 [35]	Type 4 [37]	Type 5 [38]
t_w	80	240	300	350	150
E_{wv}	1873	1873	3240	5299	6401
E_{wh}	991	991	1050	494	5038
G_w	1089	1873	1296	2120	2547
f_{wv}	2.02	1.5	3.51	4.64	8.66
f_{wlat}	1.18	1.11	1.5	1.08	4.18
f_{wu}	0.44	0.25	0.3	0.359	1.07

t_w: thickness [mm]; E_{wv}: elastic modulus vertical direction [MPa]; E_{wh}: elastic modulus horizontal direction [MPa]; G_w: shear modulus [MPa]; f_{wv}: vertical strength [MPa]; f_{wlat}: lateral strength [MPa]; f_{wu}: shear sliding strength [MPa].

Parametric nonlinear static analyses were carried out by combining the main formulations generally adopted to account for the influence of the identified parameters, and the resulting capacity curves were compared with the force-displacement curve and maximum envelope obtained from the experimental test of each masonry infill typology. The model minimizing the prediction error was finally selected for each masonry infill type. Hence, instead of selecting a priori, one of the formulations available in the literature for the definition of the hysteretic behavior of infills, the model that minimized the experimental test results prediction error was identified for each masonry infill type [18]. While the resulting backbone curves are provided in Figure 5, further details on the macro-classification, the verification that the selected infills typologies cover the range of variation of the main mechanical properties highlighted in different research studies [36,38,39], as well as the numerical modeling validation with experimental test results, can be found in Mucedero et al. [18]. Finally, according to the in situ inspection, the exterior masonry infill walls were identified as double-leaf hollow clay brick masonry, which, at least in terms of geometrical properties, can be compared with type-2 masonry infill [35] Table 1.

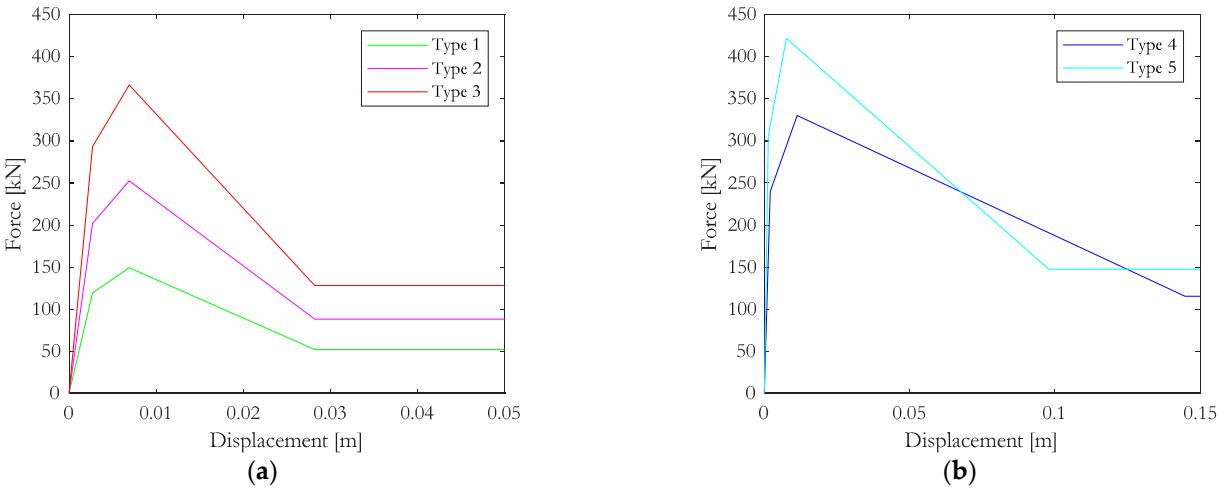

Figure 5. Backbone curves for (**a**) masonry infill types 1–2–3 and (**b**) masonry infill types 4–5.

4. Seismic Risk Assessment

The case-study school building was analyzed considering two different structural configurations: (1) completely infilled, neglecting the presence of the openings in the masonry panels, and (2) partially infilled, considering a reduction coefficient that accounts for the presence of the openings in the masonry panels, as per Decanini et al. [39], whose proposed relationship provided the best numerical fitting, for the selected masonry infills, to

experimental test results [18]. The presence of the openings, which were defined according to the real dimensions of the school building, was hence considered by multiplying the strut area obtained for the infill without opening by the aforementioned stiffness and strength reduction coefficient.

Considering the still common trend in engineering practice of considering masonry infills as non-structural components, i.e., without an explicit contribution to the structural behavior, the results of the bare frame structural configurations are also provided and compared with those of the infilled counterparts, highlighting the role and the effects of accounting for the infills in the numerical models.

The dynamic properties of the selected case-study building are summarized in Table 2 through the first four vibration modes, which allow us to clarify the importance of modeling assumptions on the dynamic behavior of the structure. The first vibration mode, T_1, varies between 1.32 s for the bare frame and 0.264 s in the case of a completely infilled frame and infill type 5 (strong infill). For both infilled configurations (1 and 2), the fundamental period decreases when moving from infill type 1 to infill type 5, as expected, which is further proof that the adopted infill typology macro-classification is not only valid in terms of strength but also in terms of stiffness. Moreover, looking at the higher modes, going from T_1 to T_4, the period of vibration starts to be less affected by the material properties of the infills, although the differences are still noticeable.

Table 2. Dynamic properties of the school building.

Structural Typology	Infill Type	T_1 [s]	T_2 [s]	T_3 [s]	T_4 [s]
Completely Infilled	1	0.644	0.471	0.388	0.238
	2	0.537	0.378	0.310	0.197
	3	0.463	0.322	0.264	0.170
	4	0.325	0.219	0.173	0.123
	5	0.264	0.171	0.131	0.094
Partially infilled	1	0.800	0.643	0.534	0.305
	2	0.682	0.520	0.437	0.259
	3	0.488	0.343	0.289	0.184
	4	0.493	0.353	0.282	0.191
	5	0.399	0.27	0.212	0.151
Bare	-	1.320	1.224	0.998	0.458

4.1. Nonlinear Static Analysis Results

The impact of the different masonry infill properties is quite visible, looking at the results of the pushover curves of the building, illustrated in Figure 6, for both directions (X and Y) and structural configurations, as a function of the masonry infill type. The seismic coefficient—base shear normalized to the total seismic weight—is quite affected by the material properties of the infills and is in the range of 0.44–0.10 and 0.43–0.095 for the completely infilled (Figure 6a,b) and partially infilled (Figure 6c,d) configurations, respectively. In particular, going from weak masonry infills to medium-strong and strong masonry infills, the seismic coefficient increases by almost 91% in the X direction and 100% in the Y direction for the completely infilled structural configuration [40]. The increment of the seismic coefficient is higher for the case in which the openings were accounted for in the numerical model, with an increment, going from weak masonry infills to medium-strong and strong masonry infills, of 168% in the X direction and 115% in the Y direction [40]. Moreover, in the case of partially infilled (Figure 6c,d), the seismic capacity decreases when compared with the completely infilled counterpart (Figure 6a,b).

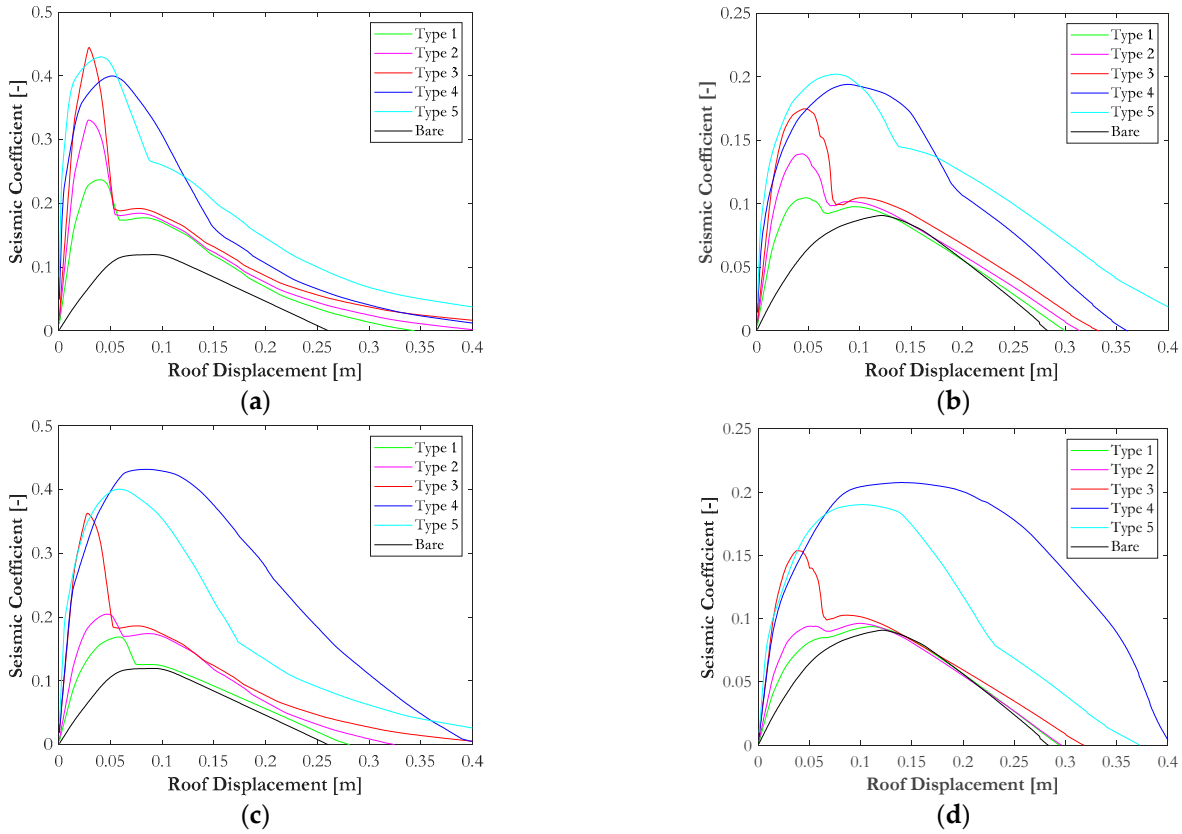

Figure 6. Normalized pushover curves for the case study school building: completely infilled configuration, (**a**) X and (**b**) Y direction, and partially infilled configuration, (**c**) X and (**d**) Y direction.

For completeness, the capacity curves for the bare frame configuration are also reported. The differences between the bare frame configuration and the infilled configuration are evident. They are less expressive only for the partially infilled configuration with weak or weak-medium infill types, as expected. It is worth noting that once most of the infills are collapsed, the post-peak branch of the pushover curves for weak and weak-medium infill types is quite close to the bare frame configuration one.

4.2. Nonlinear Time History Analysis (NTHA) Results

The response in terms of the median value of the interstorey drift ratios (MIDR) and peak floor accelerations (MPFA), along the building height, in both principal directions, is of particular interest, with a view to loss assessment. For the sake of brevity, only the results for the intensity measure (IM) level 6, which corresponds to an AvgSa ($0.1 \leq T_1$ [s] ≤ 2) of 0.28 g, are provided in Figures 7 and 8. A reduction in the MIDR (Figure 7a,b) when increasing the stiffness (also strength) of the masonry infill is highlighted. This behavior corresponds to a stiffening of the structure, as already confirmed by the results of the eigenvalue and pushover analyses. More specifically, for the IM-level 6, going from weak to strong masonry infills, the reduction of the MIDR values is in the range of [38–79%] and [22–76%] for infilled and partially infilled structural configurations, respectively. Moreover, in the case of openings, a mean increment of the MIDR values of almost 50% and 92% is observed for weak and strong masonry infills, respectively, with respect to those obtained for the infilled structural configuration.

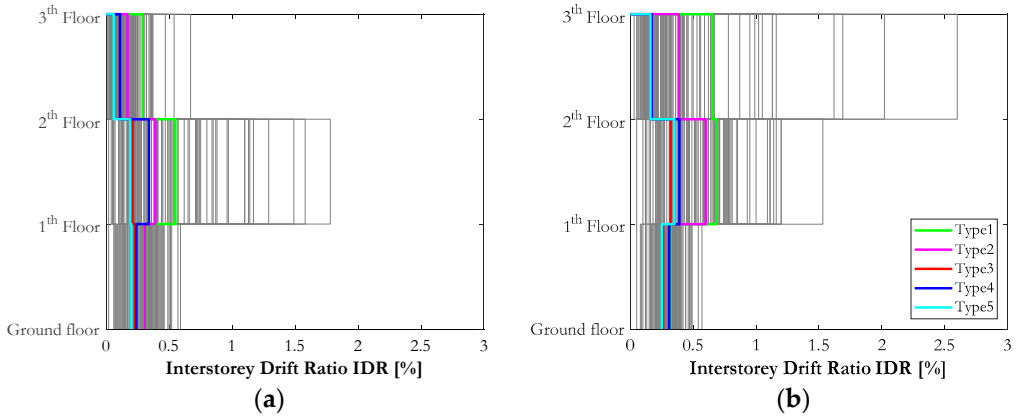

Figure 7. Median interstorey drift ratio (MIDR) profiles for the case study school building at IM level 6: (**a**) completely infilled configuration; (**b**) partially infilled configuration (X direction).

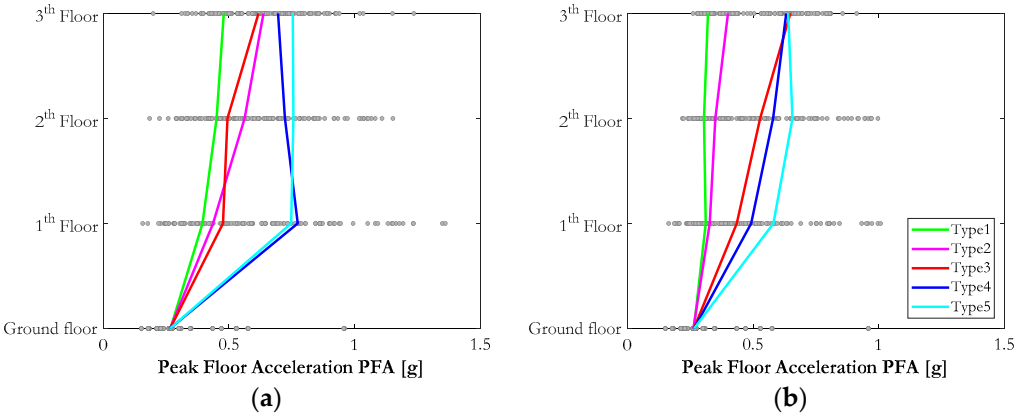

Figure 8. Median of peak floor acceleration (MPFA) profiles for the case study school building at IM level 6: (**a**) completely infilled configuration; (**b**) partially infilled configuration (X direction).

The higher values noticed for the MIDR at the first story were due to the structural characteristics of the buildings: the stiffness of this floor is quite lower than that below due to a reduction of the column cross sections along the building height.

On the other hand, looking at MPFA (Figure 8a,b), along the building height, the higher the stiffening provided by the masonry infills, the higher the recorded floor accelerations. This trend should not be generalized for every design/assessment condition, as it depends on several aspects, such as the shear capacity and deficiencies of the columns or premature shear failure due to frame-infill interaction [41,42]. In this case-study building, no premature shear failures were observed. Moreover, for the IM-level 6, going from weak to strong masonry infills, the increment of the MPFA values is in the range of [60–92%] and [87–117%] for infilled and partially infilled structural configurations, respectively. It is also worth mentioning that, in the case of openings, a mean reduction of the MPFA values of almost 29% and 17% was noticed for weak and strong masonry infills, respectively, with respect to those obtained for the fully infilled structural configuration.

4.3. Collapse Fragility Curves

The NTHA results were used to derive the collapse fragility function for each structural configuration, considering the uncertainty due to record-to-record variability. For each IM level, the number of collapses was divided by the total number of records to compute the probability of collapse. A lognormal distribution, through the maximum likelihood method outlined by Baker [43], was then fit to the collapse probability data points, leading to a median collapse intensity, θ, and a logarithmic standard deviation, β_{RTR}, associated

with the record-to-record variability, listed in Table 3, for each structural configuration. Furthermore, the fragility curves for each structural configuration are provided in Figure 9, demonstrating the high variability surrounding them when the different material properties of infills are considered.

Table 3. Collapse fragility curve parameters, as a function of both building and masonry infill typologies.

Scenario	Infill Type	ϑ [g]	β_{RTR}
Completely Infilled	1	0.50	0.20
	2	0.51	0.19
	3	0.60	0.22
	4	0.78	0.18
	5	0.85	0.17
Partially Infilled	1	0.41	0.17
	2	0.48	0.20
	3	0.53	0.22
	4	0.74	0.16
	5	0.71	0.20
Bare	-	0.33	0.13

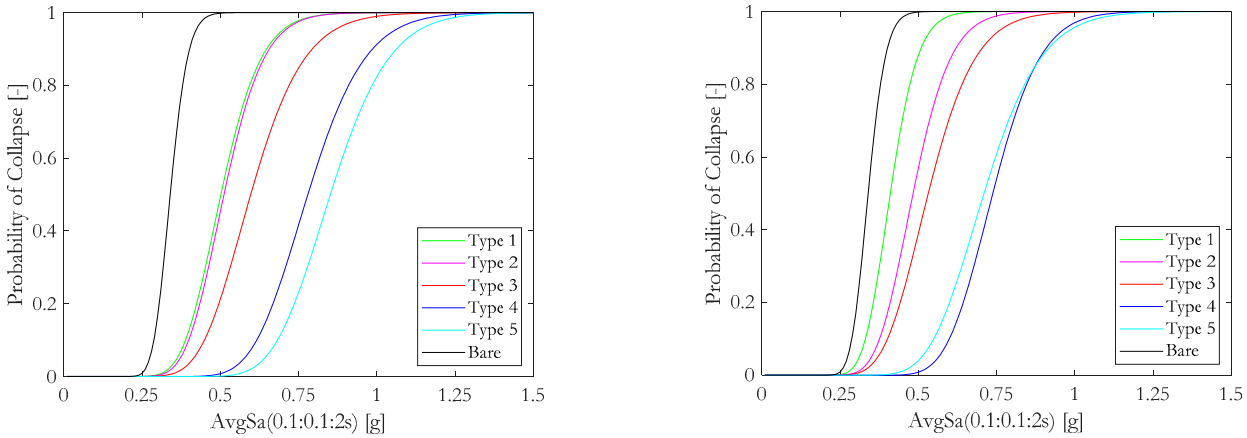

Figure 9. Collapse fragility curves for the case-study school building: (**a**) completely infilled and (**b**) partially infilled structural configurations.

The dispersion due to record-to-record variability (β_{RTR}) varies from 0.16 to 0.22, whereas the median collapse intensity (θ) can go from 0.41 g to 0.85 g. Going from weak to strong masonry infills, the median intensity of collapse increases by almost 70% in the completely infilled configuration and almost 80% in the case of the partially infilled configuration. Furthermore, the analyst's choice to account or not for the presence of openings also has a relevant impact on the fragility curves, given that accounting for the presence of openings led to a reduction of θ in the range of 5 to 18% with respect to the completely infilled structural configuration [44]. It is also worth mentioning that the trends highlighted by the fragility curves, i.e., reduction of the probability of collapse by increasing the masonry infill strength, should not be generalized. The increase in the strength of the masonry infill might induce shear failure in the columns (especially in existing buildings with poorly detailed structural components) with a consequently higher probability of collapse for the same IM level.

4.4. Seismic Loss Assessment

4.4.1. Component-Based Loss Assessment

The seismic loss estimation was carried out following the performance-based earthquake engineering (PBEE) methodology [2], which is characterized by four stages, namely: hazard and facility definition analysis, structural analysis, damage assessment, and loss analysis with quantification of repair costs. The framework requires the definition of the building components' inventory, which is related to the type of structural system, building occupancy type, and financial value of the components, amongst others. Moreover, it requires the classification of the structural and non-structural components in performance groups based on the engineering demand parameter (EDP) to which their damage is more sensitive, along with the definition of the corresponding fragility and consequence functions. The loss estimation through the PBEE methodology was carried out using the software PACT (2012) [45] for 10 return periods resulting in 200 realizations. The building components' inventory was taken from O'Reilly et al. [21] (Table 4).

Table 4. Building inventory of structural and non-structural elements, according to O'Reilly et al. [21].

List of Elements	EDP	Fragility Function	Unit	Quantities *		
				Ground	1st Floor	2nd Floor
Structural elements						
Exterior Beam-Column Joints	Drift [%]	Cardone [46]	each	20 (26)	20 (26)	20 (26)
Interior Beam-Column Joints	Drift [%]		each	23 (15)	23 (15)	22 (14)
Non-Ductile Columns	Drift [%]		each	44	44	44
Staircase	Drift [%]	FEMA P58-3 [3,45]	each	1	1	1
Masonry Infills and partition walls						
Exterior masonry infill	Drift [%]	Cardone and Perrone [47]	m^2	454.4 (2.0)	454.4 (127.8)	447.3 (125.8)
Interior masonry infill	Drift [%]	Sassun et al. [48]	m^2	198.9 (65.9)	198.9 (65.9)	195.7 (64.8)
Interior Gypsum Partitions	Drift [%]		m^2	317.8 (335.3)	291.9 (243.6)	268.1 (2 3 1)
Non-structural elements						
Doors	Drift [%]	FEMA P58-3 [3,45]	each	18 (15)	13 (10)	15 (10)
Windows	Drift [%]		each	23 (17)	50 (9)	53 (9)
Desks	Drift [%]		each	110	145	182
Chairs	Drift [%]		each	140	182	182
Ceiling System	PFA [g]		m^2	560	588	566
Fancoils	PFA [g]		each	28	30	30
Lighting	PFA [g]		each	66	48	48
Piping—Water Distribution	PFA [g]		m	452	452	452
Piping—Heating Distribution	PFA [g]		m	476	476	476
Bookcases	PFV [m/s]		each	16	22	14
Mobile Blackboards	PFA [g]		each	3	3	4
Electronic Blackboards	PFA [g]		each	0	3	3
Computers and Printers	PFA [g]		each	6	20	0
Projectors	PFA [g]		each	0	3	3
Switchboards	PFA [g]		each	1	3	3

* Quantities in the longitudinal and transverse (in brackets) directions of the school building.

In particular, the in situ surveys allowed for the accurate evaluation and quantification of all the non-structural elements in the school building; moreover, if specific information on the seismic protection of the non-structural elements was not available, they were considered without seismic design provisions.

Table 4 also includes the EDP to which the damage of each group is more sensitive (PFA for most of the non-structural elements and Peak Story Drift (PSD) for the structural components), the corresponding fragility curve, and the quantities for each story. The fragility curves proposed by Cardone [46] and FEMA P58 [3,45] for structural components were selected. In turn, for masonry infills and partition walls, the fragility functions proposed by Cardone and Perrone [47] and Sassun et al. [48] were respectively adopted, while those proposed by FEMA P58 [3,45] were assumed for all the acceleration and velocity-sensitive non-structural elements. For desks and chairs, following engineering judgment, their fragility was correlated to the fragility functions assumed for the partition walls. This assumption is corroborated by past earthquake evidence [49,50], showing how the collapse of the partition walls or infill walls would damage the adjacent desks and chairs.

Finally, according to Ramirez and Miranda [51], after a seismic event, there could be permanent lateral drifts resulting in the demolishment of the building. Hence residual drifts were also accounted for in the loss estimation by using a fragility function, with a median maximum residual story drift of 1.5% and a dispersion of 0.30.

4.4.2. Accounting for Epistemic Uncertainty

The total expected losses (LT) at different intensity levels E[LT | IM] were determined by introducing both the aleatory uncertainty, β_{RTR}, through the presented fragility models and the epistemic uncertainty, β_{MDL}, to consider the modeling uncertainties. Specifically, to account for the additional dispersion introduced via modeling uncertainty, β_{MDL}, two, as summarized in Table 5, were considered: firstly, the suggestions of O'Reilly and Sullivan [11], representing an estimate of the dispersion without the consideration of infill variability and possible RC shear failure, named herein as MDL-1. In turn, MDL-2 corresponds to the use of the more recent dispersion values proposed by Mucedero et al. [16], which include important aspects unaddressed by previous research studies, as highlighted in the Introduction section. The goal of this double approach is to investigate the impact of a more comprehensive consideration of the epistemic uncertainty dispersion on the loss assessment results. The collapse limit state MDL-1 dispersion is β_{MDL} = 0.70, whereas the MDL-2 one is β_{MDL} = 0.15. The reduction coefficients (R_f) of the median intensity of collapse, used to modify the median value when accounting for modeling uncertainty, also differ from one approach to the other, as summarized in Table 5.

Table 5. Summary of the two dispersion sets: MD-1 [13] and MDL-2 [18].

Description	Parameter	MDL-1 [11]	MDL-2 [16]
Reduction coefficient of the median intensity	R_f	0.99	0.55
Dispersion of the median intensity	β_{MDL}	0.15	0.70
Dispersion of Inter-story Drift	$\beta_{\vartheta,MDL}$	[0.15–0.40]	[0.37–0.51]
Dispersion of Peak Floor Acceleration	$\beta_{A,MDL}$	[0.15–0.90]	[0.40–0.52]

Accordingly, to indirectly account for the additional dispersion introduced via modeling uncertainty, β_{MDL}, the collapse fragility curves, the peak inter-story drift, and the peak floor acceleration demands were inflated using the Square Root Sum of the Squares (SRSS), for the two different dispersions set. It is worth mentioning that this combination could overestimate the overall dispersion due to the assumption of independency between the two sources of uncertainty [11]. The total dispersion β_T was thus obtained as in Equation (1):

$$\beta_T = \sqrt[2]{\beta_{RTR}^2 + \beta_{MDL}^2} \quad (1)$$

4.4.3. Results

Figure 10 depicts the vulnerability curves, i.e., the expected total losses normalized with respect to the total replacement cost (3,929,937 €) for the completely infilled (Figure 10a) and partially infilled (Figure 10b) structural configurations. Moreover, the mean (η) and the dispersion (±σ) of the vulnerability curves, obtained when considering the five masonry infill types, are presented for both dispersion sets (MDL-1 and MDL-2).

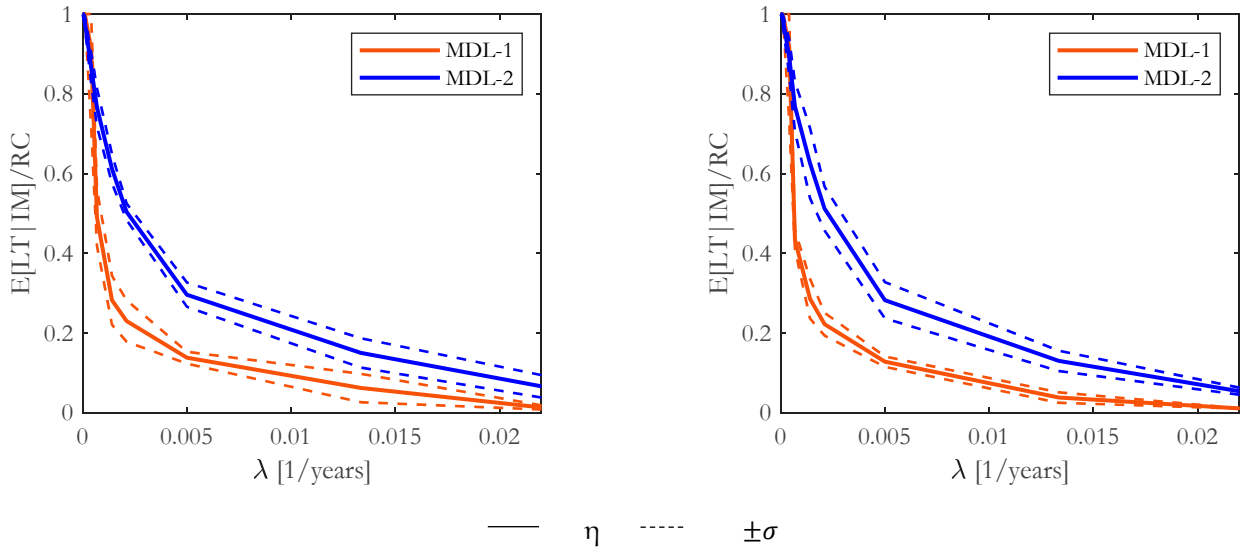

Figure 10. Vulnerability curves: (**a**) completely and (**b**) partially infilled structural configurations.

The more recent dispersion values employed in this study, as per Mucedero et al. [16], confirmed higher loss ratios with respect to those taken from previous studies (O'Reilly and Sullivan [11]), regardless of the presence or not of the openings; however, the difference in terms of loss ratio is higher in case of infilled frames with openings. Furthermore, the standard deviation of the loss ratio is in the range of [0.004–0.2] and [0.02–0.05] for the infilled frames with the MDL-1 and MDL-2 dispersion values, respectively. In case of infilled frames with openings, the standard deviation of the loss ratio, respectively for MDL-1 and MDL-2, is in the range of [0.01–0.18] and [0.01–0.09].

The resulting expected annual losses (EAL) are presented in Figure 11 as a function of the masonry infill typology and modeling approach (with or without openings). Since the presence of the masonry infills has proven to increase the PFA and reduce the IDR, as discussed in Di Domenico et al. [52] and Mucedero et al. [41], an additional distinction was made, in terms of component groups: (1) both drift- and acceleration-sensitive components were considered in the non-structural components inventory; (2) only drift-sensitive components were considered in the non-structural components inventory. This catered for a better understanding of the effects of masonry infill properties on the loss estimation, as well as how much the different dispersion components (β_{MDL}, $\beta_{\vartheta,MDL,}$ and $\beta_{A,MDL}$) affect the estimation of EALs.

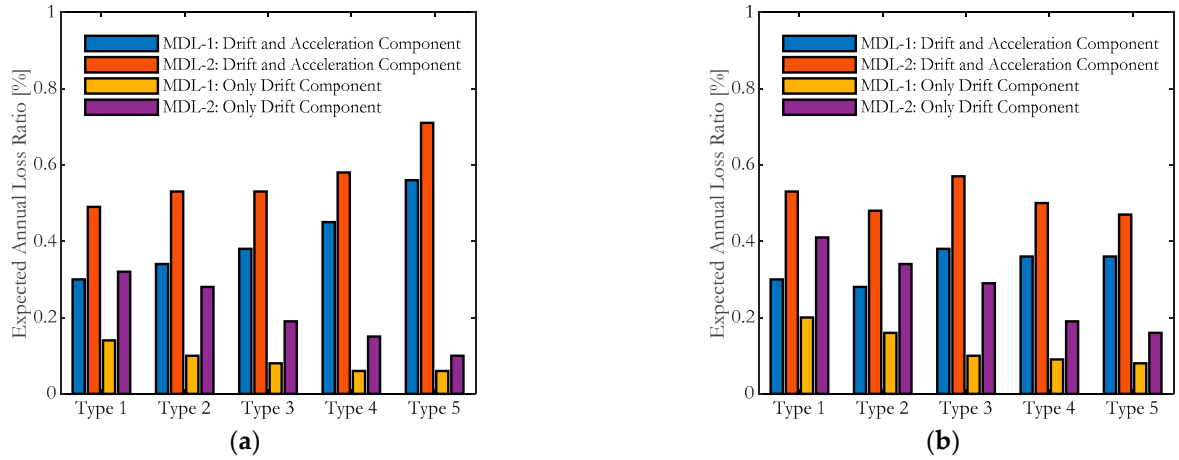

Figure 11. Expected annual loss (EAL) ratios considering the two sets of dispersion values for both drift- and acceleration-sensitive non-structural components or only drift-sensitive non-structural components: (**a**) completely and (**b**) partially infilled structural configurations.

For what concerns the infilled frames (Figure 11a), when both drift and acceleration-sensitive components are considered, using the MDL-2 dispersion [16], the EALs are 1.3 to 1.6 times higher than those obtained with the MDL-1 dispersion [11], with the lowest difference occurring for strong masonry infills (type-5). The EAL always increases when going from weak to strong masonry infills. When the presence of openings is accounted for (Figure 11b), the same MDL-2/MDL-1 EAL ratio increases to the range of [1.3–1.8]; on the other hand, for the case completely infilled, no particular trend for the total EAL, as a function of the macro-classification of the infills, is observed. This could be due to the reduction of stiffness and strength, which is used to account for the presence of the openings, leading to a different structural response of the building when compared with the uniformly infilled typology.

If only drift-sensitive non-structural components are considered for both structural configurations and dispersion values proposed, the EAL reduces substantially with the increase in strength of strong masonry infills. This result denotes that although the increase in the stiffness, or strength, of the masonry panel, leads to a reduction of damage/collapse of non-structural drift-sensitive components, the EAL related to acceleration-sensitive components increases much more (especially for very stiff masonry infills). Overall, considering the updated dispersion set suggested in Mucedero et al. [16], MDL-2, the mean increment of EAL, when both acceleration- and drift-sensitive components are considered, is 61% and 49% for the completely and partially infilled frames, respectively. The corresponding standard deviation is close to 20% for both structural configurations considered.

Finally, to further gauge the effects of modeling uncertainty on the loss estimation, a disaggregation in terms of drift- and acceleration-sensitive components was performed. The results are provided in Figure 12, in which the outcomes obtained using MDL-1 and MDL-2 are compared. The disaggregated results show, firstly, that for weak (type-1) and weak to medium (type-2) masonry infills, the major contribution to EAL is given by drift-sensitive components, and, therefore, the MDL-2 EAL for drift-sensitive components is much higher than that of MDL-1. Secondly, increasing the stiffness of the masonry infills, the difference between MDL-1 and MDL-2-based EALs is much lower for drift-sensitive components. Conversely, the impact of the higher-dispersion MDL-2 is quite notable, especially for medium and strong masonry infills, on the losses related to acceleration-sensitive components, with respect to MDL-1. In turn, for acceleration-sensitive components and weak (type-1) and weak-to-medium (type-2) masonry infills, the differences between MDL-1 and MDL-2 are negligible for both structural configurations. Finally, the impact of different dispersion values and the reduction coefficient of the median intensity is quantified in

Figure 13. The median increment of the EAL ratio, with respect to the MDL-1 values, is 28% and 33%, without and with openings, respectively.

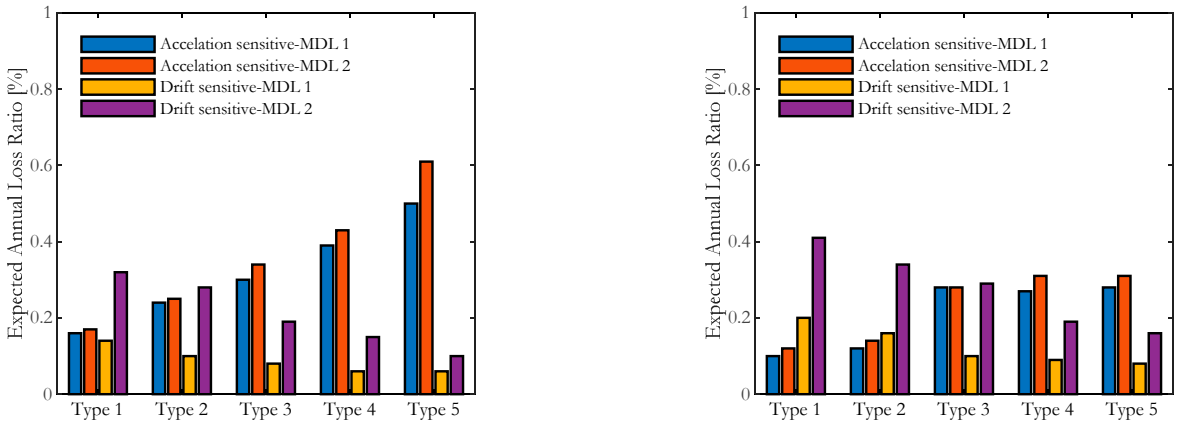

Figure 12. Disaggregation of the expected annual losses as a function of the non-structural components typology and the two sets of dispersion values: (**a**) completely and (**b**) partially infilled structural configurations.

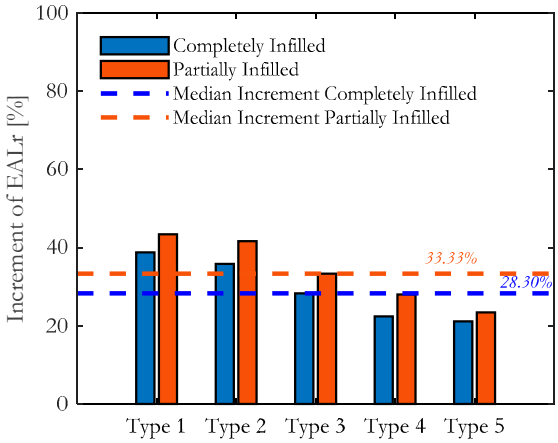

Figure 13. Increment of the expected annual losses ratio of MDL-1 [11] with respect to MDL-2 [16].

5. Conclusions

Although many efforts have been made in the last years to demonstrate the influence of masonry infills on the seismic performance of RC buildings, no particular attention has been paid to the variability surrounding the mechanical properties of masonry infills and how this might affect the uncertainty in fragility and loss estimation. Even in cases where the masonry infills have been considered through simplified approaches, the variability related to the geometrical configuration, material properties, and modeling assumptions was not explicitly considered. This study dealt with the effects of epistemic uncertainty and different masonry infill typologies on loss assessment of masonry-infilled existing RC buildings. The dispersion values recently proposed in the literature were used to perform a detailed loss assessment of an Italian RC existing school building and compared with the loss values obtained with other epistemic uncertainty-based dispersion proposals available in the literature. The main conclusions can be summarized as follows:

- The capacity curves and the results in terms of EDPs, i.e., Interstorey Drift Ratio and Peak Floor Acceleration, are strongly affected by the masonry infill variability. In addition, the dynamic properties of the building could be highly influenced by the material properties of the masonry, with a lengthening or shortening of the first period

of vibration, also influenced by the choice of accounting or not for the presence of the openings. As such, proper identification of the material and geometrical properties of masonry infills should be made to perform a reliable seismic assessment of the building;

- In all the cases for which no information on the material properties of the infills is available, the macro-level classification presented herein could support analysts in selecting, beforehand, what models could be more representative of the actual nonlinear response of the masonry infill typology;
- Accounting for the presence of the infill openings led to a reduction of the median intensity of collapse in the range of 5 to 18% with respect to the completely infilled structural configuration. Regarding the role of accounting for the presence of openings on the EAL, it was highlighted that the EAL estimation could be underestimated or overestimated by up to 50% with respect to the completely infilled counterparts as a function of the masonry infill typologies and the typology of non-structural components. As such, the presence of openings should be absolutely contemplated in the models;
- Reliable identification and propagation of uncertainty in the collapse assessment of existing structures is of paramount importance, and consequently, the loss estimation is quite affected by the assumed epistemic uncertainty: the EALs obtained with the updated epistemic set are 1.3 to 1.8 times higher than those obtained with the previous one;
- The impact of modeling uncertainty on the EAL estimations did depend on the typology of structural and non-structural components considered in the inventory group as a function of the masonry infill type. Indeed, the differences in the EALs obtained when using the two dispersion sets are negligible for the acceleration-sensitive components and weak (type-1) and weak-to-medium (type-2) masonry infills. On the other hand, the impact of the higher dispersion introduced by MDL-2 is quite noticeable for medium and strong masonry infills. For drift-sensitive components, the higher impact of modeling uncertainty is observed for the weak (type-1) and weak-to-medium (type-2) masonry infills, while it is negligible for medium and strong masonry infills;
- When the dispersion is quantified considering the uncertainty related to the variability in masonry infills and the premature shear failure of RC columns due to the interaction with the infill panels, a higher loss ratio with respect to the available literature approaches is obtained, regardless of the presence or not of the openings in the infill panels. Such a median increase in EAL, if up to 30%, was observed;
- A loss disaggregation in terms of acceleration- and drift-sensitive components has also confirmed how increasing the stiffness of the masonry panels leads to an equally noticeable increase in the losses related to acceleration-sensitive non-structural components due to higher floor accelerations. This shows how the presence of one infill type over one other can significantly alter the structural response of the building and the level of expected losses;
- A reasonable EAL estimation should include the most accurate level of knowledge regarding both the structural system and the masonry infill properties, which proved to largely increase the levels of epistemic uncertainty when considering the variability of their mechanical properties and their possible induction of RC column shear failure.

Author Contributions: Conceptualization, R.M.; methodology, G.M., D.P. and R.M.; software, G.M.; validation, G.M., D.P. and R.M.; formal analysis, G.M.; investigation, G.M., D.P. and R.M.; data curation, G.M., D.P. and R.M.; writing—original draft preparation, G.M.; writing—review and editing, D.P. and R.M.; supervision, D.P. and R.M.; funding acquisition R.M. All authors have read and agreed to the published version of the manuscript.

Funding: The work presented in this paper has been developed within the framework of the project "ReLUIS 2022-2024," funded by the Italian Civil Protection Department at IUSS Pavia.

Institutional Review Board Statement: Not applicable.

Informed Consent Statement: Not applicable.

Data Availability Statement: The data presented in this study is available upon request.

Conflicts of Interest: The authors declare no conflict of interest.

References

1. Borzi, B.; Ceresa, P.; Faravelli, M.; Fiorini, E.; Onida, M. Seismic Risk Assessment of Italian School Buildings. *Comput. Methods Appl. Sci.* **2013**, *30*, 317–344. [CrossRef]
2. Cornell, C.A.; Krawinkler, H. Progress and Challenges in Seismic Performance Assessment. *PEER Center News* **2003**, *3*, 1–3.
3. Federal Emergency Management Agency. *FEMA P-58: Seismic Performance Assessment of Buildings, Volume 2—Implementation Guide*, 2nd ed.; 2018; Volume 2. Available online: https://femap58.atcouncil.org/ (accessed on 18 October 2022).
4. De Angelis, A.; Pecce, M. Seismic Nonstructural Vulnerability Assessment in School Buildings. *Nat. Hazards* **2015**, *79*, 1333–1358. [CrossRef]
5. Grant, D.N.; Bommer, J.J.; Pinho, R.; Calvi, G.M.; Goretti, A.; Meroni, F. A Prioritization Scheme for Seismic Intervention in School Buildings in Italy. *Earthq. Spectra* **2007**, *23*, 291–314. [CrossRef]
6. Borzi, B.; Ceresa, P.; Faravelli, M.; Fiorini, E.; Onida, M.; Borzi, B.; Ceresa, P.; Faravelli, M.; Fiorini, E.; Onida, M. Definition of a Prioritisation Procedure for Structural Retrofitting of Italian School Buildings. In Proceedings of the COMPDYN 2011 III ECCOMAS Thematic Conference on Computational Methods in Structural Dynamics and Earthquake Engineering, Corfu, Greece, 25–28 May 2011.
7. Haselton, C.B.; Goulet, C.A.; Mitrani-Reiser, J.; Beck, J.L.; Deierlein, G.G.; Porter, K.A.; Stewart, J.P.; Taciroglu, E. *An Assessment to Benchmark the Seismic Performance of a Code-Conforming Reinforced Concrete Moment-Frame Building*; PEER Report 2007/1; Pacific Earthquake Engineering Research Center: Berkeley, CA, USA, 2008; 360p. Available online: https://resolver.caltech.edu/CaltechAUTHORS:20120831-144606048 (accessed on 18 October 2022).
8. Baker, J.W.; Cornell, C.A. Uncertainty Propagation in Probabilistic Seismic Loss Estimation. *Struct. Saf.* **2008**, *30*, 236–252. [CrossRef]
9. Lee, T.H.; Mosalam, K.M. Seismic Demand Sensitivity of Reinforced Concrete Shear-Wall Building Using FOSM Method. *Earthq. Eng. Struct. Dyn.* **2005**, *34*, 1719–1736. [CrossRef]
10. Liel, A.B.; Haselton, C.B.; Deierlein, G.G.; Baker, J.W. Incorporating Modeling Uncertainties in the Assessment of Seismic Collapse Risk of Buildings. *Struct. Saf.* **2009**, *31*, 197–211. [CrossRef]
11. O'Reilly, G.J.; Sullivan, T.J. Quantification of Modelling Uncertainty in Existing Italian RC Frames. *Earthq. Eng. Struct. Dyn.* **2018**, *47*, 1054–1074. [CrossRef]
12. Olsson, A.; Sandberg, G.; Dahlblom, O. On Latin Hypercube Sampling for Structural Reliability Analysis. *Struct. Saf.* **2003**, *25*, 47–68. [CrossRef]
13. Choudhury, T.; Kaushik, H.B. Treatment of Uncertainties in Seismic Fragility Assessment of RC Frames with Masonry Infill Walls. *Soil Dyn. Earthq. Eng.* **2019**, *126*, 105771. [CrossRef]
14. Crisafulli, F.J.; Carr, A.J. Proposed Macro-Model for the Analysis of Infilled Frame Structures. *Bull. New Zealand Soc. Earthq. Eng.* **2007**, *40*, 69–77. [CrossRef]
15. Crisafulli, F. Seismic Behaviour of Reinforced Concrete Structures with Masonry Infills. Ph.D. Thesis, University of Canterbury, Canterbury, New Zealand, 1997.
16. Mucedero, G.; Perrone, D.; Monteiro, R. Epistemic Uncertainty in Poorly Detailed Existing Frames Accounting for Masonry Infill Variability and RC Shear Failure. *Earthq. Eng. Struct. Dyn.* **2022**, *51*, 3755–3778. [CrossRef]
17. Mucedero, G.; Perrone, D.; Monteiro, R. Nonlinear Static Characterisation of Masonry—Infilled RC Building Portfolios Accounting for Variability of Infill Properties. *Bull. Earthq. Eng.* **2021**, *19*, 2597–2641. [CrossRef]
18. Mucedero, G.; Perrone, D.; Brunesi, E.; Monteiro, R. Numerical Modelling and Validation of the Response of Masonry Infilled Rc Frames Using Experimental Testing Results. *Buildings* **2020**, *10*, 182. [CrossRef]
19. Chrysostomou, C.Z.; Gergely, P.; Abel, J.F. A Six-Strut Model for Nonlinear Dynamic Analysis of Steel Infilled Frames. *Int. J. Struct. Stab. Dyn.* **2002**, *2*, 335–353. [CrossRef]
20. Puppio, M.L.; Giresini, L.; Doveri, F.; Sassu, M. Structural Irregularity: The Analysis of Two Reinforced Concrete (r.c.) Buildings. *Eng. Solid Mech.* **2019**, *7*, 13–34. [CrossRef]
21. O'Reilly, G.J.; Perrone, D.; Fox, M.; Monteiro, R.; Filiatrault, A. Seismic Assessment and Loss Estimation of Existing School Buildings in Italy. *Eng. Struct.* **2018**, *168*, 142–162. [CrossRef]
22. Perrone, D.; O'Reilly, G.J.; Monteiro, R.; Filiatrault, A. Assessing Seismic Risk in Typical Italian School Buildings: From in-Situ Survey to Loss Estimation. *Int. J. Disaster Risk Reduct.* **2020**, *44*, 101448. [CrossRef]
23. Mazzoni, S.; McKenna, F.; Fenves, G.L. Open System for Earthquake Engineering Simulation (OpenSees). Available online: https://opensees.berkeley.edu/wiki/index.php/Main_Page (accessed on 18 October 2022).
24. Scott, M.H.; Fenves, G.L. Plastic Hinge Integration Methods for Force-Based Beam–Column Elements. *J. Struct. Eng.* **2006**, *132*, 244–252. [CrossRef]

25. Carofilis, W.; Perrone, D.; O'Reilly, G.J.; Monteiro, R.; Filiatrault, A. Seismic Retrofit of Existing School Buildings in Italy: Performance Evaluation and Loss Estimation. *Eng. Struct.* **2020**, *225*, 111243. [CrossRef]
26. O'Reilly, G.J.; Perrone, D.; Fox, M.; Monteiro, R.; Filiatrault, A.; Lanese, I.; Pavese, A. System Identification and Seismic Assessment Modeling Implications for Italian School Buildings. *J. Perform. Constr. Facil.* **2019**, *33*. [CrossRef]
27. Silva, V.; Crowley, H.; Pagani, M.; Monelli, D.; Pinho, R. Development of the OpenQuake Engine, the Global Earthquake Model's Open-Source Software for Seismic Risk Assessment. *Nat. Hazards* **2014**, *72*, 1409–1427. [CrossRef]
28. Giardini, D.; Wössner, J.; Danciu, L. Mapping Europe's Seismic Hazard. *EOS* **2014**, *95*, 261–262. [CrossRef]
29. Boorea, D.; Atkinson, G. Ground-Motion Prediction Equations for the Average Horizontal Component of PGA, PGV, and 5%-Damped PSA at Spectral Periods between 0.01 s and 10.0 s. *Earthq. Spectra* **2008**, *24*, 99. [CrossRef]
30. Kohrangi, M. Beyond Simple Scalar Ground Motion Intensity Measures for Seismic Risk Assessment. Ph.D. Thesis, University School for Advance Studies, IUSS Pavia, Pavia, Italy, 2015.
31. Kohrangi, M.; Vamvatsikos, D.; Bazzurro, P. A Record Selection Methodology for Vulnerability Functions Consistent with Regional Seismic Hazard for Classes of Buildings. In Proceedings of the 16th World Conference on Earthquake Engineering, Santiago, Chile, 9–13 January 2017.
32. Ancheta, T.D.; Darragh, R.B.; Stewart, J.P.; Seyhan, E.; Silva, W.J.; Chiou, B.S.J.; Wooddell, K.E.; Graves, R.W.; Kottke, A.R.; Boore, D.M.; et al. *PEER NGA-West2 Database, Technical Report PEER 2013/03*; Pacific Earthquake Engineering Research Center, University of California: Berkeley, CA, USA, 2013.
33. Luzi, L.; Lanzano, G.; Felicetta, C.; D'Amico, M.C.; Russo, E.; Sgobba, S.; Pacor, F. *ORFEUS Working Group 5. ESM—The Engineering Strong-Motion Database*; Istituto Nazionale di Geofisica e Vulcanologia (INGV): Rome, Italy, 2020. Available online: https://data.ingv.it/it/dataset/418#additional-metadata (accessed on 18 October 2022).
34. NTC-2018. *Aggiornamento Delle « Norme Tecniche per Le Costruzioni»*; Supplemento Ordinario n. 8 Alla Gazzetta Ufficiale Del 20-2-2018; MIT: Rome, Italy, 2018; Volume 20. (In Italian)
35. Hak, S.; Morandi, P.; Magenes, G. Prediction of Inter-Storey Drifts for Regular RC Structures with Masonry Infills Based on Bare Frame Modelling. *Bull. Earthq. Eng.* **2018**, *16*, 397–425. [CrossRef]
36. Calvi, G.M.; Bolognini, D. Seismic Response of Reinforced Concrete Frames Infilled with Weakly Reinforced Masonry Panels. *J. Earthq. Eng.* **2001**, *5*, 153–185. [CrossRef]
37. Morandi, P.; Hak, S.; Magenes, G. Performance-Based Interpretation of in-Plane Cyclic Tests on RC Frames with Strong Masonry Infills. *Eng. Struct.* **2018**, *156*, 503–521. [CrossRef]
38. Cavaleri, L.; di Trapani, F. Cyclic Response of Masonry Infilled RC Frames: Experimental Results and Simplified Modeling. *Soil Dyn. Earthq. Eng.* **2014**, *65*, 224–242. [CrossRef]
39. Decanini, L.D.; Liberatore, L.; Mollaioli, F. Strength and Stiffness Reduction Factors for Infilled Frames with Openings. *Earthq. Eng. Eng. Vib.* **2014**, *13*, 437–454. [CrossRef]
40. Mucedero, G.; Carofilis, W.; Perrone, D.; Monteiro, R. Impact of Masonry Infill Properties and Modelling Uncertainty on the Seismic Risk Assessment of Existing Italian School Buildings. In Proceedings of the ICOSSAR 2021–2022, 13th International Conference on Structural Safety & Reliability, Shanghai, China, 13–17 September 2022.
41. Mucedero, G.; Perrone, D.; Brunesi, E.; Monteiro, R. Impact of Masonry Infill Variability on the Estimation of Floor Response Spectra in Rc Buildings. In Proceedings of the 8th International Conference on Computational Methods in Structural Dynamics and Earthquake Engineering Methods in Structural Dynamics and Earthquake Engineering, Athens, Greece, 27–30 June 2021; pp. 27–30. [CrossRef]
42. Mucedero, G.; Perrone, D.; Monteiro, R. Seismic Risk Assessment of Masonry-Infilled RC Building Portfolios: Impact of Variability in the Infill Properties. *Bull. Earthq. Eng.* **2022**. [CrossRef]
43. Baker, J.W. Efficient Analytical Fragility Function Fitting Using Dynamic Structural Analysis. *Earthq. Spectra* **2015**, *31*, 579–599. [CrossRef]
44. Mucedero, G.; Perrone, D.; Monteiro, R. Epistemic uncertainty impact on seismic loss estimates of an Italian RC existing school building. In Proceedings of the 3th European Conference on Earthquake Engineering & Seismology, Bucharest, Romania, 4–9 September 2022.
45. Federal Emergency Management Agency (FEMA). *P-58-3, Seismic Performance Assessment of Buildings: Volume 3—Performance Assessment Calculation Tool (PACT)*; FEMA: Washington, DC, USA, 2012.
46. Cardone, D. Fragility Curves and Loss Functions for RC Structural Components with Smooth Rebars. *Earthq. Struct.* **2016**, *10*, 1181–1212. [CrossRef]
47. Cardone, D.; Perrone, G. Developing Fragility Curves and Loss Functions for Masonry Infill Walls. *Earthq. Struct.* **2015**, *9*, 257–279. [CrossRef]
48. Sassun, K.; Sullivan, T.J.; Morandi, P.; Cardone, D. Characterising the In-Plane Seismic Performance of Infill Masonry. *Bull. New Zealand Soc. Earthq. Eng.* **2016**, *49*, 98–115. [CrossRef]
49. Braga, F.; Manfredi, V.; Masi, A.; Salvatori, A.; Vona, M. Performance of Non-Structural Elements in RC Buildings during the L'Aquila, 2009 Earthquake. *Bull. Earthq. Eng.* **2011**, *9*, 307–324. [CrossRef]
50. Tsionis, G.; Bossi, A.; Pinto, A.; Marazzi, F. *The L'Aquila (Italy) Earthquake of 6 April 2009: Report and Analysis from a Field Mission*; Publications Office of the European Union: Luxembourg, 2011; ISBN 9789279189906.

51. Ramirez, C.M.; Miranda, E. *Building Specific Loss Estimation Methods & Tools for Simplified Performance Based Earthquake Engineering*; Blume Report No. 171; Blume Earthquake Engineering Research Center: Stanford, CA, USA, 2009.
52. Di Domenico, M.; Ricci, P.; Verderame, G.M. Floor Spectra for Bare and Infilled Reinforced Concrete Frames Designed According to Eurocodes. *Earthq. Eng. Struct. Dyn.* **2021**, *50*, 3577–3601. [CrossRef]